

FORMULAE FOR PREDICTING STRESS CONCENTRATION FACTORS IN FLAT PLATES AND CYLINDRICAL PRESSURE VESSELS WITH HOLES: A REVIEW

P. K. NZIU & L. M. MASU

Department of Mechanical Engineering, Vaal University of Technology, South Africa

ABSTRACT

A review of formulae used for predicting Stress Concentration Factors (SCFs) in both flat plate and cylindrical pressure vessels with holes was conducted. The SCF solutions for a flat plate with a hole are affected by the plate length, thickness, the cross bore diameter, geometric dimensions of the discontinuities and the elastic constants. However, there was no available information on an optimal solution for a flat plate with a hole. On the other hand, the solutions for SCFs at the tee junction of a thin cylindrical shell depends on geometric parameters such as the ratio of diameter, thickness, and other physical characteristics at the junction such as sharp corners, chamfers and blades. Noticeably, there was no universally accepted solution for determining SCFs at these tee junctions. Besides, most of the reviewed solutions for the cross bored thick walled cylinders were only able to predict SCFs at the intersection between the cross bore and the main bore. Though other reviewed studies had proven that maximum SCF does not necessarily occur at the cross bore intersection, but slightly away from the cross bore intersection. Therefore, there is a need to develop formulae that can predict SCFs magnitudes at an optimal position along the cross bore.

KEYWORDS: Stress Concentration Factors, Formulae, Solutions, Flat Plates, Cylindrical Vessels, Holes & Cross Bores

Received: Jun 11, 2019; **Accepted:** Jul 02, 2019; **Published:** Sep 23, 2019; **Paper Id.:** IJMPERDOCT201967

INTRODUCTION

Stress concentration is caused by the presence of any form of discontinuity in a structure. A discontinuity can either be in the form of load, metallurgical, geometrical or a combination thereof, alter the otherwise uniform stress distribution across the structure (Nziu and Masu, 2019a). This alteration of uniform stress distribution leads to the creation of high stress concentration particularly in the neighbourhood regions of the discontinuity (Cole *et al.*, 1976).

Stress concentration is measured using different types of dimensionless factors. The classification of these types of dimensionless factors varies with the type of discontinuity and the working conditions of the structure, among other considerations (Nziu and Masu, 2019b). For geometrical discontinuity, such as holes, cavities, notches, fillets and grooves, this stress factor is referred to as Stress Concentration Factor (SCF) (Ford and Alexander, 1977). Besides, high magnitudes of SCF have been linked to the cause of most failures in structural engineering design such as fatigue, fracture and premature yielding (Nziu and Masu, 2019c). As a result, SCF remains one of the important parameters to be determined in any engineering design (Kihui, 2002).

Over the years, numerous studies have been conducted using analytical, experimental and numerical methods to develop formulae for predicting SCF in cylindrical pressure vessels (Nziu and Masu, 2019a). With assumption that a flat plate is a section of a cylinder with an infinite radius (Makulsawatudom *et al.*, 2004), different analytical formulae have been developed for predicting SCF in cylindrical pressure vessels.

Standard formulae are used to provide the much-needed information during the design of pressure vessels with holes, particularly in development of engineering design standards. This lead to the realization of manufacturing benefits such as safe working environments, improved equipment availability and reliability, economic use of materials, low operating costs as well as a reduction in losses as a result of either catastrophic or disruptive failures (Masu, 1989).

Therefore, this study seeks to review formulae used for predicting SCFs in both flat plate and cylindrical pressure vessels with holes. Since the ultimate engineering goal is to design for minimum SCF, the methods used for SCF reduction will fall within the ambit of this paper.

STRESS CONCENTRATION ANALYSES

Theoretical SCF is calculated using the relationship shown in Equation (1) (Ford and Alexander, 1977, Masu, 1997; Masu, 1998);

$$\text{SCF} = \frac{\text{Maximum hoop stress at a point due to the introduction of a discontinuity}}{\text{Corresponding hoop stress at the same point without a discontinuity}} \quad (1)$$

This particular definition of SCF gives the intensity of stress concentration intensity at each point of interest. Other authors, especially in the area of thin cylindrical vessels field, refer to SCF as Effective Stress Factor (ESF) (Moffat *et al.*, 1991).

Various solutions for SCFs have been developed for flat plates with holes, as well as in high-pressure cylindrical vessels having radial, offset and inclined holes. A brief review of existing formulae is presented under the following sub headings

Solutions for SCFs in flat plates with Circular or Elliptical Holes

Solutions for SCFs of flat plates with circular holes under tension as shown in Figure 1, have been developed and are widely used in engineering and machine design. Nagpal *et al.* (2012) cited Kirsch's analytical solutions for radial σ_{rr} , hoop $\sigma_{\theta\theta}$, and shear $\tau_{r\theta}$ stresses for large thin flat plates with a small circular hole at the centre, under uniaxial tension applied at the far field as:

$$\sigma_{rr} = \frac{\sigma}{2} \left(1 - \frac{a^2}{r^2} \right) + \frac{\sigma}{2} \left(1 - \frac{a^2}{r^2} \right) \left(1 - \frac{3a^2}{r^2} \right) \cos 2\theta \quad (2)$$

$$\sigma_{\theta\theta} = \frac{\sigma}{2} \left(1 + \frac{a^2}{r^2} \right) - \frac{\sigma}{2} \left(1 + \frac{3a^4}{r^4} \right) \cos 2\theta \quad (3)$$

$$\tau_{r\theta} = -\frac{\sigma}{2} \left(1 - \frac{a^2}{r^2} \right) - \frac{\sigma}{2} \left(1 + \frac{3a^2}{r^2} \right) \sin 2\theta \quad (4)$$

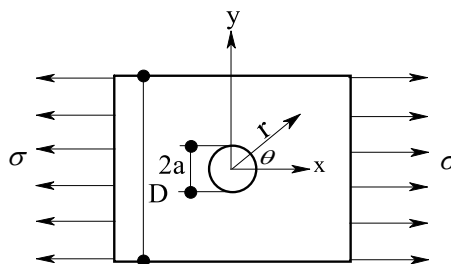


Figure 1: Flat Thin Plate with Central Small Circular Holes under Tension (Dharmin *et al.*, 2012).

where

σ is the far-field uniaxial tension, θ is the subtended angle measured clockwise from X-axis and a is the radius of the circular hole. Equations 2 to 4 are analytical equations for an infinitely small circular hole in a plate also referred to as the Kirsch's solutions. The maximum SCF with a magnitude of 3 occurs at an angle of 90° at the radius of the hole. However, in the derivation of these equations 2 – 4, the ratio of the hole radius, a , and the plate width, b , was neglected ($\frac{a}{b} \sim 0$). Despite the assumption, these equations were found to give sufficiently accurate results when the ratio of $\frac{a}{b} < \frac{1}{10}$ (Ford and Alexander, 1977).

The solution for SCF for a flat plate with the same features as those discussed in the preceding paragraph was presented by Hyder and Asif (2008) using two equations. For $\frac{d}{w} \leq 0.65$ the solution was given as;

$$SCF = 3.0039 - 3.753 \frac{d}{w} + 7.9735 \left(\frac{d}{w}\right)^2 - 9.2659 \left(\frac{d}{w}\right)^3 + 1.8145 \left(\frac{d}{w}\right)^4 + 2.9684 \left(\frac{d}{w}\right)^5 \quad (5)$$

while for $\frac{d}{w} > 0.65$ as;

$$SCF = 2.0 + \left(1 - \frac{d}{w}\right)^3 \quad (6)$$

where 'd' is the hole diameter and w is the width of the plate

However, the SCF solution curves generated by the two equations had a discontinuity at the point where the ratio of $\frac{d}{w} = 0.65$.

Nagpal *et al.*, (2012) reported that further studies by various researchers based on existing experimental and analytical data for flat plates with holes led to the development of a single equation for calculating the solution of SCF. This eliminated the discontinuity posed by equations 5 and 6, earlier discussed. The solution of SCF for a flat plate with a circular cross bore was given as;

$$SCF = 3.0 - 3.13 \left(\frac{2r}{w}\right) + 3.66 \left(\frac{2r}{w}\right)^2 - 1.53 \left(\frac{2r}{w}\right)^3 \quad (7)$$

where

$2r$ is the hole diameter and w is the width of the plate

It can be seen from equations 5, 6 and 7 that, the SCF is a function of the hole diameter and the width of the plate.

Snowberger (2008) gave the solution for SCF of a flat plate with an elliptical hole as;

$$SCF = C1 + C2 \left(\frac{2a}{w}\right) + C3 \left(\frac{2a}{w}\right)^2 + C4 \left(\frac{2a}{w}\right)^3 \quad (8)$$

Where

$$C1 = 1.0 + 2 \left(\frac{a}{b}\right)$$

$$C2 = -0.351 - 0.021 \sqrt{\left(\frac{a}{b}\right)} - 2.483 \left(\frac{a}{b}\right)$$

$$C3 = 3.621 - 5.183 \sqrt{\left(\frac{a}{b}\right)} + 4.494 \left(\frac{a}{b}\right)$$

$$C4 = -2.27 + 5.204 \sqrt{\left(\frac{a}{b}\right)} - 4.011 \left(\frac{a}{b}\right)$$

a is the major axis of the ellipse, b is the minor axis of the ellipse and w is the plate width

In addition, this study by Snowberger (2008) proved the validity of equation 8 from the known exact analytical solution of a circle, as the elliptical bore approached a circular shape.

Another study by Nihous *et al.* (2008) cited a closed-form solution for predicting SCF in a thin plate under biaxial loading having either circular or elliptical hole given by;

$$SCF = 0.5 + 2 \frac{b}{a} \quad (9)$$

Where a and b are the diameters of an elliptical hole along the direction of the applied loads σ_0 and $\sigma_0/2$, respectively. However, equation 9 was noted to give a constant SCF magnitude of 2.5 for all circular holes regardless of their size.

Further reviewed literature by Nagpal *et al.* (2012) indicated that the SCF in flat plates was affected by plate length, thickness, hole size, geometric dimensions of the discontinuities and the elastic constants. In another study by Makulsawatudom *et al.*, (2004), on a simple finite plate with a hole under uniaxial loading, it was established that the SCF increases with increasing hole size. The study attributed this occurrence to the effects of through-thickness. However, there was no available information on an optimal solution for a flat plate with a hole.

Methods of Reducing SCF in Flat Plates with Holes

Small holes in both sides of the main hole commonly referred to as auxiliary holes have been introduced in the design of flat plates with holes to reduce SCFs as shown in Figure 2. These auxiliary holes cause stress redistribution around the vicinity of the main hole. These hole arrangements create regions of smooth flow stress trajectories which in turn lead to reduced SCF.

Heywood (1952) studied various methods for the reduction of SCFs. The study reported a reduction of 16% in SCFs after the introduction of a single auxiliary hole in the main hole axis. Erickson and Riley (1978) carried out another study on minimisation of SCFs around circular holes. The optimum centre distance between the hole and the auxiliary hole was found to be 14.4 mm when the main hole and auxiliary holes' diameters were 42.9 mm and 11.1 mm, respectively. They reported a reduction of SCF ranging from 13 to 21%.

Another similar study by Sanyal and Yadav (2006) developed formulae for calculating the optimum size of the auxiliary hole and the centre distance between the hole and the auxiliary hole. The Sanyal and Yadav formulae for optimum conditions are presented as;

$$a_2 = 0.85a_1 \quad (10)$$

where

a_1 is the main hole radius, a_2 is the auxiliary hole radius

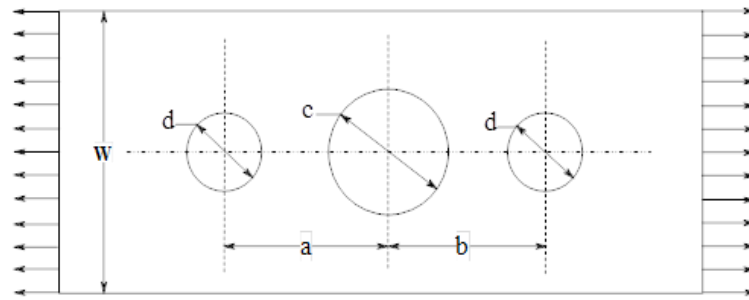


Figure 2: Flat Plate with Main and Auxiliary Circular Holes (Erickson and Riley, 1978).

$$\delta = \sqrt{3a_1 + a_2} \quad (11)$$

where, δ is the optimum centre distance

The study reported that the use of the Sanyal and Yadav formulae, the SCF was reduced by 17%. However, a disparity of the results given by the two studies discussed earlier occurred when the optimum values of the auxiliary hole given by Erickson's and Riley's (1978) study were tested on Sanyal and Yadav (2006) formulae.

Further literature reviewed by Nagpal *et al.* (2012) on flat plates with holes, revealed that introducing 2 or 3 co-axial circular auxiliary holes in the cross bore axis, also termed as defence hole system method, reduce SCFs by 7.5 to 11 %. The authors also reported that SCFs can be reduced by using composite material rings or laminate plates around the cross bore as a form of material reinforcement. The presence of material rings and laminates alter the stress distribution around the cross bore vicinity. Moreover, the study also revealed that gradual increase of the Young's modulus of elasticity away from the cross bore centre had a reducing effect on SCFs. The review concluded that the reduction of SCFs mainly depended on the size and location of the auxiliary hole. However, the study did not consider the effects of various auxiliary hole shapes in stress reduction citing initial design constraints as well as thickness ratios and angles of inclination.

SOLUTIONS FOR SCFS IN CYLINDRICAL PRESSURE VESSELS WITH HOLES

Many terminologies are used to describe the nature of holes or openings constructed in the wall of cylindrical pressure vessels. These holes are commonly referred to as cross bore (Masu and Craggs, 1992; Peter, 2003). Whenever a cross bore is positioned at the censorial axis of the cylinder is known as radial cross bore (Nziu and Masu, 2019c). Whereas, offset cross bores refers to laying of the cross bore in any other chord away from the censorial axis. On the other hand, oblique or inclination of cross bores refers to placing cross bores in the longitudinal axis of the cylinder (Nziu and Masu, 2019a). These terminologies are illustrated in Figures 3 to 5.

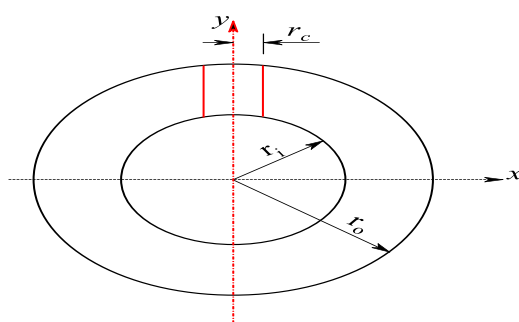


Figure 3: Radial Cross Bore.

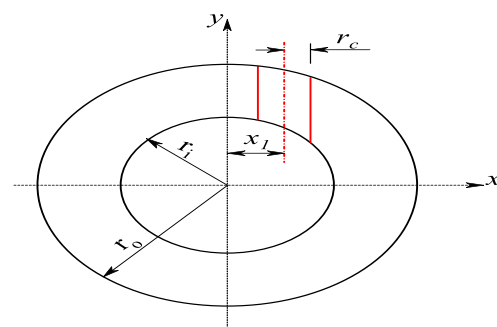


Figure 4: Offset Cross Bore.

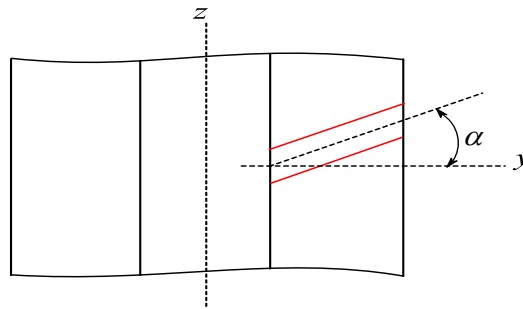


Figure 5: Oblique Cross Bore.

Where r_c is the radius of the cross is bore, r_i is the internal radius of the main bore, r_o is the external radius of the main bore, x_1 is the offset distance and α is the oblique angle.

Further study by Nziu and Masu (2019d) indicated that only circular and elliptical shaped cross bores are commonly used in the design of pressure vessels. A circular cross bore is termed as being small when the ratio of the cross bore to main bore diameter is ≤ 0.5 . Nonetheless, when the same bore ratio lies between ≥ 0.5 and ≤ 1 the cross bore is termed as large.

On the other hand, an elliptical cross bore is described in the form of diameters ratios and their orientation with the principal stress axes. According to Nziu and Masu (2019e) study, an optimal configuration of elliptical cross bore in both thin and thick walled cylinder has diameter ratio of 2 when the orientation of the minor diameter is parallel to the axial direction of the cylinder.

A review of formulae used in predicting SCF in cylindrical pressure vessel with holes is presented under the following four sub sections

Solutions for SCF in Thick Cylinders with Radial Cross Bores

Various solutions have been developed to calculate SCF in high-pressure vessels with small and large circular cross bores. Earliest researchers developed solutions by considering a cylinder with a cross bore as a flat plate with a small elliptical hole at the centre, under tension. The circumference and the height of the cylinder are considered as the plate width and height, respectively. Timoshenko (1940) cited SCF as;

$$SCF = 1 + \frac{2a}{b} \quad (12)$$

Where 'a' is the ellipse semi-major axis (m) and 'b' is the ellipse semi-minor axis (m).

In this approach, it was assumed that the width of the plate is large compared to the semi-major axis, a. In the case of a circular hole (where $a = b$), the SCF was found to be 3. However, the results arising from a further experimental and theoretical analysis conducted by Faupel and Harris (1957) on equation 12, failed to support this analysis.

Fessler and Lewin (1956) studied stress distribution in a tee junction of thick pipes. They assumed cylindrical thin plate sheets as infinite flat plates each with a circular hole under the action of internal pressure and two perpendicular tensions. These perpendicular tensions are the corresponding hoop and axial stresses that could have acted on the pipe as if the tee junction did not exist. They presented an analytical solution for SCF of closed-end pipes as;

$$SCF = \frac{4R_2^2 + R_1^2}{R_2^2 + R_1^2} \quad (13)$$

where

R_1 is the inside radius of the pipe and R_2 is the outside radius of the pipe

Faupel and Harris (1957) derived the same equation as Fessler and Lewin's by considering an elliptical hole in an infinite elastic plate subjected to tensile loading. For a circularly shaped cross bore, an SCF equal to 2.5 was obtained; a decrease of 16.7% from that of equation 12. The reduction was due to the effects of longitudinal stresses generated by the closed ends of the cylinder. However, the derivation of equation 13 did not take into account the shear and compressive stresses which occur within the cross bore vicinity.

The results obtained using equation 13 gave an error that was 32% greater than experimental results, performed by photo elastic methods. The photo elastic experiment was performed on a cross bored cylinder with diameter ratios of 3, and the ratio of the cylinder bore to the cross bore as 2. This meant that the size of the cylinder used for the test was too large for equation 13 to be applicable (Cheng, 1978). O'Hara (1968) conducted another similar study using the method of photo elasticity. The study considered two cross bored cylinders having diameter ratios of 1.75 and the ratio of the main bore to cross bore diameter as 10 and 20. They reported SCFs of 2.95 and 2.75, respectively, which were 14% less than those given by equation 12.

Further study of equation 13 was carried out by Comlekci *et al.*, (2007). They investigated the elastic stress concentration using Finite Element Analysis (FEA) on radial cross holes in pressurised thick cylinders with cylinder diameter ratio ranging from 1.4 to 2.5. They concluded that equation 13 gave results with an accuracy of up to 99 % for only small holes. These small holes had the ratio of the main cylinder bore to that of the cross bore diameter ≤ 100 .

Various solutions for determining the SCF in large cross bores have also been developed. Faupel and Harris (1957) presented a solution for the SCF of large circular cross bores using experimental data from Peterson Stress Intensification Factors Charts. The intensification factors α and γ are used to calculate SCF as shown in equation 14. The values of intensification factors for various side hole ratios as compiled by Faupel and Harris (1957) are tabulated in Table~1.

The solution of SCF proposed by Faupel and Harris (1957), using intensification factors, is presented as;

$$SCF = \frac{\alpha\sigma_h + \gamma\sigma_z}{\sigma_h} \quad (14)$$

Where

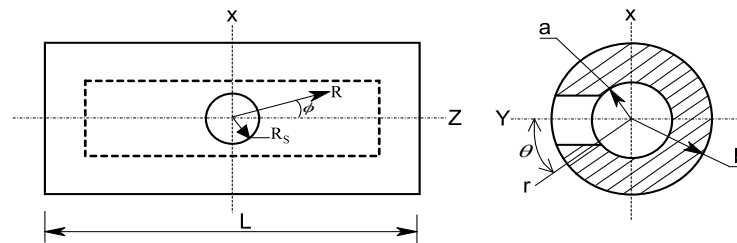
σ_h is the hoop stress at the surface of the cross bore, σ_z is the longitudinal stress at the surface of the cross bore, α and γ is the intensification factors.

However, there was no information given on intensification factors for other cross bore profiles such as elliptical and notches.

Gerdeen (1972) presented lengthy analytical solutions for calculating SCFs for large cross bores, which were referred to as side holes. The coordinates and dimensions used for the SCF analysis are shown in Figure 6.

Table 1: Peterson Stress Intensification Factors (Faupel and Harris, 1957)

Side Hole Ratio ($\frac{\text{Cylinder bore radius}}{\text{Cross bore radius}}$)	α	γ
10	3.00	-0.92
9	3.00	-0.90
8	3.00	-0.88
7	2.96	-0.86
6	2.95	-0.84
5	2.92	-0.81
4	2.88	-0.77
3	2.82	-0.70
2	2.71	-0.58
1	2.57	-0.33

**Figure 6. Coordinates and Dimensions of the Cylinder with A Cross Bore (Gerdeen, 1972).**

A simplified technique to be followed for calculating the SCF using Gerdeen's method is summarised hereunder;

- Determination of hoop stress for a cylinder without a hole using Lamé's theory.
- Determination of the total surface stresses at the cylinder bore necessary to keep internal pressure constant. The surface stresses at the cross bore are the sum of radial σ_{RR} and shear stresses $\tau_{R\phi}$ and τ_{RY} in the transverse plane required to keep the internal stresses constant as in a cylinder without cross bore. The two components of shear stresses were calculated in polar coordinates at the Y-axis and a subtended angle θ from the Y-axis
- Determination of hoop stress, $\sigma_{\phi\phi}$ at the intersection. This was obtained by subtracting the results of (ii) from (i).
- Determination of the internal pressure, p in the cylinder.

The maximum hoop stress at the cross bore intersection is obtained by summing the results of (i), (iii) and (iv). The SCF at the intersection is then calculated using equation 1.

However, this study did not take into consideration the stresses in the longitudinal plane. Despite Gerdeen's method giving an approximate solution, it considered the effects of shear stress which had been previously neglected by other researchers.

Solutions for SCFs in Thin Cylindrical Shells with Radial Cross Bores

A study by Xie and Lu, (1985) reported that most solutions developed using theoretical methods were limited to thin-walled cylinders with the ratio of cross bore to main bore $\leq \frac{1}{3}$. This limitation was associated with difficulties in mathematical analysis. A review by Moffat *et al.*, (1999), compiled SCFs for 36 different geometric sizes at the pipe branch junction under internal pressure loading carried out by different studies. The stress analysis in these studies was performed using experimental and numerical Finite Element Analysis (FEA) methods. The SCFs and their respective geometric dimensions are summarised in Tables 2 and 3.

Table 2: SCFs at the Pipe Branch Junction Performed by Experimental Method (Moffat *et al.*, 1999)

S/No.	d/D	D/T	t/T	SCF
1	0.20	8.00	0.20	3.25
2	0.22	15.80	0.43	3.20
3	0.24	19.50	0.54	2.80
4	0.25	16.50	0.57	3.40
5	0.29	12.90	0.49	4.60
6	0.31	17.90	0.40	3.40
7	0.55	21.00	1.82	2.70
8	0.55	57.60	0.91	4.90
9	0.62	9.98	0.62	4.75
10	0.62	15.08	1.00	3.70
11	0.64	19.00	0.69	5.00
12	0.66	18.87	0.64	4.53
13	0.69	156.00	0.63	8.00
14	0.76	10.30	1.50	3.50
15	1.00	19.00	1.00	5.40
16	1.00	24.70	1.00	4.18

Table 3: SCFs at the Pipe Branch Junction Performed by FEA Method (Moffat *et al.*, 1999)

S/No.	d/D	D/T	t/T	SCF
1	0.09	36.06	1.13	2.55
2	0.12	49.00	0.84	2.52
3	0.16	10.30	0.22	3.14
4	0.20	8.00	0.20	3.25
5	0.22	9.00	0.30	3.01
6	0.22	16.65	0.45	3.20
7	0.39	10.84	0.41	3.87
8	0.46	5.50	1.00	2.44
9	0.50	2.33	0.50	3.62
10	0.50	3.50	0.50	3.63
11	0.50	7.67	0.50	4.17
12	0.50	11.00	0.50	4.23
13	0.62	9.98	0.62	4.24
14	0.62	15.08	1.00	3.60
15	0.64	7.00	0.70	4.10
16	0.70	16.00	0.75	4.67
17	0.80	20.00	1.00	4.08
18	0.91	7.00	0.96	4.35
19	1.00	4.70	1.00	2.80
20	1.00	17.94	1.00	4.03

Where d , is the branch pipe diameter, D is the run pipe diameter, t is the branch pipe thickness and T is the run pipe thickness.

Most of the SCF analysis reviewed in tables 2 and 3 were performed on vessels with large openings. The experimental work was done using full-scale models. Generally, the data presented in these two tables were found to be consistent and have been used in other previous studies (Qadir and Redekop, 2009) as a reference guideline. The term “reference standard” will be used in this work to refer to the data in tables 2 and 3.

Lind (1967) studied stress concentration in pressurised pipe connection branches and developed two solutions for calculating SCFs using area replacement mathematical techniques. The solution for SCF was taken to be the maximum value obtained from these two equations as shown by equation 15.

$$SCF = \text{Max} \left\{ \begin{array}{l} \frac{\left[1 + 1.77 \left(\frac{d}{D} \right) \sqrt{\frac{D}{T}} + \left(\frac{d}{D} \right)^2 \sqrt{\frac{s}{S}} \right] \left[1 + \frac{T/D}{\sqrt{s/S}} \right]}{1 + \frac{\left(\frac{d}{D} \right)^2}{\frac{s}{S} \sqrt{s/S}}} \dots \dots \dots (15 a) \\ \frac{\left[1.67 \sqrt{s/S} \cdot \sqrt{D/T} + 0.565 \left(\frac{d}{D} \right) \right] \left[1 + \frac{(T/D)}{\sqrt{s/S}} \right]}{0.67 \sqrt{s/S} \sqrt{D/T} + 0.565 \frac{(d/D)}{s/S}} \dots \dots \dots (15 b) \end{array} \right. \quad (15)$$

where

$$s = d/2t$$

$$S = D/2T$$

t is the nozzle thickness, d is the nozzle mean diameter, D is the vessel main diameter and T is the vessel thickness

Qadir and Redekop (2009) studied SCFs at the nozzle intersection in a pressurised vessel using the FEA. They compared the results obtained by Lind's equation at the intersection with those from the reference standard given by Moffat *et al.* (1999). The study reported that the results given by Lind's equation had a standard deviation of 1.77 from the reference standard and classified them as being conservative.

Money (1968) developed two other solutions for SCF analysis using linear regression analysis based on several experimental data on tee joints, performed using the method of photo elasticity. The solutions of SCF developed by Money are presented here as;

$$SCF = 2.5 \left[\left(\frac{r}{t} \right) \frac{2T}{R} \right]^{0.2042} \text{ for } 0 < r/R \leq 0.7 \quad (16)$$

$$SCF = 2.5 \left[\left(\frac{r}{t} \right) \frac{2T}{R} \right]^{0.24145} \text{ for } 0.7 \leq r/R \leq 1.0 \quad (17)$$

where

r is the vessel mean radius, R is the nozzle mean radius, t is the nozzle thickness and T is the vessel thickness

The two equations are seen to be dependent on the ratio of cross bore and cylinder bore diameters. However, the solutions present two separate curves with a discontinuity when the ratio of $(r/R) = 0.7$. Hence there was no definite solution when the ratio of $(r/R) = 0.7$.

Qadir and Redekop (2009) and Moffat *et al.*, (1991) further studied the two Money's equations and reported a standard deviation of 0.811 from the reference standard. They termed the results obtained from the two equations as accurate.

Decock (1975) developed another solution for SCFs based on experimental data conducted on a pipe branch using strain gauges and the method of photo elasticity. The solution for SCF was given as;

$$SCF = \frac{\left[2 + 2\frac{d}{D}\sqrt{\left(\frac{d}{D}\times\frac{t}{T}\right)} + 1.25\frac{d}{D}\sqrt{\frac{D}{T}} \right]}{\left[1 + \frac{t}{T}\sqrt{\left(\frac{d}{D}\times\frac{t}{T}\right)} \right]} \quad (18)$$

where

t is the nozzle thickness, d is the nozzle mean diameter, D is the vessel main diameter and T is the vessel thickness

The Decock equation was further studied by Moffat *et al.*, (1991) who reported that the equation gave accurate results when the ratio of cylinder diameter and thickness was equal to 20. However, they reported erroneous results when the ratio was above or below 20. Consequently, Qadir and Redekop (2009) reported a standard deviation of 1.482 from the reference standard and recommended the use of Decock's equation in determining SCFs at the crotch corner of a tee joint. They termed the results given by the equation as being conservative.

Xie and Lu (1985) developed a three term polynomial solution for predicting SCFs in cylindrical pressure vessels with nozzles using the least squares method. The three term polynomial solution was fitted using experimental data. The solution for SCFs is given as

$$SCF = 2.87 + \left[1.38 - 0.72 \left(\frac{t}{T} \right)^{0.5} \right] \left(\frac{D}{T} \right)^{0.43} \left(\frac{d}{D} \right)^{0.9} - \left(\frac{t}{T} \right)^{0.5} \quad (19)$$

where

D is the mean diameter of the vessel, d is the mean diameter of the nozzle, T is the wall thickness of the vessel and t is the wall thickness of the nozzle

The accuracy of the Xie and Lu's solution was validated using Money's, Decock's and Lind's solutions at the tee pipe junction. The study reported that Xie and Lu's equation had the best accuracy of 87%, in comparison to Decock's (83.2%), Lind's (72.3%) and Money's (70.7%). Further, the authors recommended the use of the Xie and Lu's solution in the determination of SCFs for both small and large openings.

Moffat *et al.* (1999) derived a lengthy polynomial function using several geometric parameters to determine the SCF on a tee junction using three dimensional FEA. Their solution is presented here as;

$$SCF = \left[a_1 + a_2 \left(\frac{d}{D} \right) + a_3 \left(\frac{d}{D} \right)^2 + a_4 \left(\frac{d}{D} \right)^3 \right] + \left[a_5 + a_6 \left(\frac{d}{D} \right) + a_7 \left(\frac{d}{D} \right)^2 + a_8 \left(\frac{d}{D} \right)^3 \right] \left(\frac{t}{T} \right) + \left[a_9 + a_{10} \left(\frac{d}{D} \right) + a_{11} \left(\frac{d}{D} \right)^2 + a_{12} \left(\frac{d}{D} \right)^3 \right] \left(\frac{D}{T} \right)^P + \left[a_{13} + a_{14} \left(\frac{d}{D} \right) + a_{15} \left(\frac{d}{D} \right)^2 + a_{16} \left(\frac{d}{D} \right)^3 \right] \left(\frac{t}{T} \right) \left(\frac{d}{T} \right)^P \quad (20)$$

where

t is the nozzle thickness, d is the nozzle mean diameter, D is the vessel main diameter, T is the vessel thickness and P = 1.2

The constants a_1 to a_{16} were obtained from the 3D FEA and given as 2.5, 2.715, 8.125, -6.877, -0.5, -1.193, -5.416, 5.2, 0.0, 0.078, -0.195, 0.11, 0.0, -0.043, 0.152 and -0.097.

Later, Qadir and Redekop (2009) studied the Moffat *et al.* (1999) equation and reported a standard deviation of 0.903 from the reference standard. They termed the results given by the equation as being accurate.

Table 4: Comparison of Standard Deviation Calculated in Reference to the Standard

Author	Standard deviation
Lind (1967)	1.77
Money (1968)	0.811
Decock (1975)	1.482
Moffat <i>et al.</i> , (1999)	0.903
Gurumurthy <i>et al.</i> , (2001)	1.721

Gurumurthy *et al.*, (2001) following a similar procedure as Moffat *et al.* (1991), developed a simplified solution for SCF at the nozzle shell junction based on shell theory using FEA. The solution for SCFs obtained was given as;

$$SCF = 1.75(T/t)^{0.4} (d/D)^{-0.08} (\lambda)^{0.6} \quad (21)$$

where

$$\lambda = d/(DT)^{0.5} \text{ (Pipe factor)}$$

t is the nozzle thickness, d is the nozzle mean diameter, D is the vessel main diameter and T is the vessel thickness

The authors compared the solution of this equation with those of Money (1967), Decock (1975) and Moffat *et al.* (1999) and reported some discrepancies in the SCF values obtained. However, despite the discrepancies, the authors recommended the use of Gurumurthy's equation for stress intensity approximation. In the same study, conducted by Qadir and Redekop (2009), they reported that solutions obtained from the Gurumurthy's equation had a standard deviation of 1.721 from the reference standard. They termed the results as being more conservative, with greater fluctuations than those from other methods discussed earlier.

Only Decock (1975) and Money (1968) equations gave lowest standard deviation in reference to the standard indicating acceptable degree of accuracy.

Solutions for SCFs in Thick Cylinders with Offset Cross Bores

Little and Bagci (1965) study reported that whenever a small offset cross bore is positioned along the radial X-axis of the cylinder, it resembles an ellipse when viewed from the intersection of the main bore and the cross bore. The study attributed this occurrence due to curvilinear nature of the cylinder. This phenomenon is demonstrated in Figure 7 hereunder

Cheng (1978) cited the analytical solution of SCF for closed end cylinder at the ends of the major axis as;

$$SCF = \frac{2(C-1)R_2^2 + R_1^2}{R_2^2 + R_1^2} \quad (22)$$

while at the end of the minor axis as;

$$SCF = \frac{\left(4R_2^2/C\right) + R_1^2}{R_2^2 + R_1^2} \quad (23)$$

where

C- Ratio of the major and minor axis of the formed ellipse (Ellipticity) R1- Cylinder inside radius and R2- Cylinder outside radius Comparing the two equations, it was evident that the SCF at the major axis is higher than that of the minor axis.

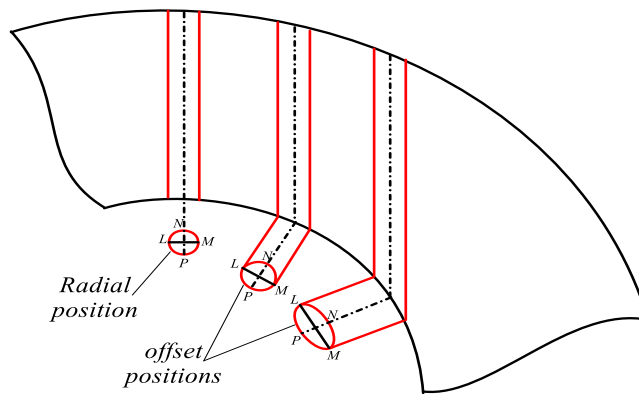


Figure 7. Images of Radial and Offset Cross Bores when Viewed at the Intersection of the Main Bore (Masu, 1998).

On the other hand, equations 24 and 25 are used to predict SCF in open cylinders at the end of major and minor axes, respectively. The symbol notations remain the same as in the preceding equations.

$$SCF = \frac{2(C-1)R_2^2 - 2CR_1^2}{R_2^2 + R_1^2} \quad (24)$$

$$SCF = \frac{\left(\frac{4R_2^2}{C}\right) + 2R_1^2}{R_2^2 + R_1^2} \quad (25)$$

Solutions for SCFs in Thick Cylinders with Oblique Cross Bores

Similar to the preceding sections, whenever small oblique circular cross bores are drilled in the longitudinal plane of the cylinder, the holes resemble an ellipse when viewed from the intersection of main bore and cross bore. The maximum SCF occurs only at the ends of the major axis. Equations 26 and 27 are used to determine the maximum SCF for open and closed thick cylinders, respectively.

$$SCF = \frac{4CR_2^2 + 2R_1^2}{R_2^2 + R_1^2} \quad (26)$$

$$SCF = \frac{4CR_2^2 + R_1^2}{R_2^2 + R_1^2} \quad (27)$$

The symbol notations remain the same as those given in equations 22 and 23.

Notably, the SCF given by the closed cylinder equation is lower than that of the open cylinder, an occurrence attributed to the generation of axial stresses by the end enclosures, unlike in the latter. It is worth to note those equations 22 to 27 only predict SCF at the intersection of the cross bore and the main bore. However, other reviewed studies (Masu, 1989; Kihui, 2002; Masu 1997; Masu 1998; Makulsawatudom *et al.*, 2004) have shown that maximum SCF does not necessarily occur at the intersection. But slightly away from the cross bore intersection. Besides, there is no any available information on experimental or numerical validation of these equations.

Methods of Reducing SCF in Cross Bored Pressure Vessels

Methods used to reduce stress concentration in cross bored pressure vessels are influenced by the geometric parameters of the cross bore such as the size, shape, location, obliquity and the vessel thickness. Most of the reviewed studies on the

reduction of SCF are centered on the effects of chamfers, blades and radii on cross bores in cylinders with various thickness ratios (Makulsawatudom *et al*, 2004). In addition, different cross bore sizes and shapes at both radial and offset positions have also been studied. Other techniques such as offsetting of circular cross bore have been reported to give lower SCF (Nziu and Masu, 2019d). Whereas, positioning of elliptical shaped cross bore at radial position gives the lowest SCF (Nziu and Masu, 2019e). However, formulae for predicting SCFs at these optimal positions are not exhaustive, especially when the position of maximum hoop stresses does not occur at the intersection between the cross bore and the main bore. In this regards, therefore, there is need to develop more formulae that are able to predict SCFs along the cross bore at different locations.

SUMMARY AND DISCUSSIONS

Various solutions for SCFs have been developed for flat plates with holes and high pressure vessels having radial and inclined cross bores. The SCF of a flat plate with a hole is affected by the plate length, thickness, the cross bore diameter, geometric dimensions of the discontinuities and the elastic constants. Introduction of circular auxiliary small holes in flat plates with the main hole reduced SCFs by a maximum of 21%. However, the existing methods used in SCFs reduction did not consider the effects of other design parameters such as shape, thickness ratio and angle of inclination. A big disparity was noted on the two solutions given by Erickson and Riley (1978) and Sanyal and Yadav (2006) studies. Probably due to the assumptions made during the development of the respective solutions. Besides, there was no available information on an optimal solution for a flat plate with a hole.

Of all the reviewed solutions for predicting SCFs in cylindrical cross bored pressure vessels, none gave the optimal location of the cross bore. Besides, equations 12 and 13 is derived analytically, the authors did not take into consideration the analysis of hoop, radial and shear stress arising from the cross bore cross section when viewed from the longitudinal plane. Moreover, it was also noted that there was no universally accepted solution for calculating the SCFs.

From table 4, it is evident that reliable and correct results for predicting SCF in thin cylindrical shells are given by equations 16, 17 and 20 which had an approximate standard deviation of 0.9 from the reference standard. Despite solution validation of equation 19, the reviewed literature did not show any extensive application on other studies. The solutions for SCFs at the tee junction of a thin cylindrical shell depend on geometric parameters such as the ratio of diameter, thickness, and other physical characteristics at the junction such as sharp corners, chamfers and blades. Noticeably, there was no universally accepted solution for determining SCFs at these tee junctions.

The magnitude of SCFs as observed from this review depend mainly on design parameters such as angle of inclination, cross bore size, position, shape, and thickness ratio. However, formulae for predicting SCFs at different optimal locations are not exhaustive. Therefore, there is a need to develop more formulae those can predict SCFs along the cross bore.

CONCLUSIONS

The SCF solution for flat plate with a hole was found to be affected by the plate length, thickness, cross bore diameter, geometric dimensions of the discontinuities and the elastic constants. However, there was no available information on an optimal solution for a flat plate with a hole. On the other hand, the solutions for SCFs at the tee junction of a thin cylindrical shell depend on geometric parameters such as the ratio of diameter, thickness, and other physical characteristics at the junction such as sharp corners, chamfers and blades.

Noticeably, there was no universally accepted solution for determining SCFs at the tee junction. In addition, most of the reviewed formulae for cross bored thick cylinders are only able to predict SCFs at the intersection between the cross bore and the main bore. In contrast, other reviewed studies had shown that maximum hoop stress does not necessarily occur at the intersection, but slightly away from the cross bore intersection. To this end, therefore, there is need to develop formulae that are able to predict optimal position of SCFs along the cross bore at different offset positions.

ACKNOWLEDGEMENTS

This research work was supported by Vaal University of Technology. The authors wish to thank the department of Mechanical Engineering at Vaal University of Technology for facilitating this work.

REFERENCES

1. Cheng, Y. F. (1978), "Stress concentration around inclined holes in pressurized thick-walled cylinders" Technical Report - Arlcb-TR-78019.
2. Cole, B. N., Craggs, G., and Ficenec, I. (1976), "Strength of cylinders containing radial or offset cross-bores", *Journal mechanical engineering science*, Vol. 18, No. 6.
3. Comlekci, T., Mackenzie, D., Hamilton, R. and Wood, J. (2007), "Elastic stress concentration at radial crossholes in pressurized thick cylinders, *Journal of strain analysis*, Vol. 42, pp, doi. Org/10.1243/03093247JSA251
4. Decock, J. (1975), "Reinforcement method of openings in cylindrical pressure vessels subjected to internal pressure", *Centre de Recherches Scientifiques et Techniques de L'Industrie des Fabrications Metalliques*, Report No. MT 104.
5. Dharmin, P., Khushbu, P. and Chetan, J. (2012), "A review on stress analysis of an infinite plate with cut-outs", *International journal of scientific and research publications*, Vol. 2, issue 11.
6. Mohsin, N. R. (2015). *Comparison between Theoretical and Numerical Solutions for Center, Single Edge and Double Edge Cracked Finite Plate Subjected to Tension Stress. International Journal of Mechanical and Production Engineering Research and Development (IJMPERD)*, 5(2), 11–20.
7. Erickson, P. E. and Riley, W. F. (1978), "Minimizing stress concentration around circular holes in uniaxially loaded plates", *experimental mechanics*, Vol 18, No.3, pp. 97–100.
8. Faupel, J. H. and Harris, D. B. (1957), "Stress concentration in heavy-walled cylindrical pressure vessels", *Industrial and engineering chemistry*, Vol. 49, pp. 1979–1986.
9. Fessler, H. and Lewin, B. H. (1956), "Stress distribution in a tee-junction of thick pipes", *British journal of applied physics*, Vol. 7, pp. 76–79.
10. Ford, H. and Alexander, J. (1977), "Advanced mechanics of materials", John Wiley and sons inc., Canada, second edition.
11. Gerdeen J. C. (1972), "Analysis of stress concentration in thick cylinders with sideholes and crossholes", *Trans. ASME, Journal Engineering Industry*, No. 94, pp. 815–823.
12. Al-Qutaiti, Y., & Ahmad, I. (2018). *EFL Supervisors' Perspectives towards Students' Insufficient Repertoire in the Omani Governmental Schools: Causes and Solutions. International of Research in Applied, Natural and Social Sciences*, 6 (11), 9, 22.
13. Gurumurthy K., Jain R and Salpekar, V. Y. (2001), *Simplified formula for stress concentration factor in radial nozzle shell junctions under internal pressure loading*, *ASME PVP- 430*, 3–6.
14. Heywood, R. B. (1952), "Designing by photoelasticity, Chapman & Hall Ltd., London, 296–298.

15. Hyder, J. M. and Asif, M. (2008), "Optimization of location and size of opening in a pressure vessel cylinder using ANSYS", *Engineering failure analysis*, Vol.15, pp. 1–19.
16. Kihiu, J. M. (2002), "Numerical stress characterization in cross bored thick walled cylinders under internal pressure", *The University of Nairobi, PhD thesis*.
17. Chatziangelou, m., Thomopoulos, a., & Christaras, b. *Excavation and Supported Solutions for the Unexpected Failure Conditions at Symvolo Mountain tunnel Construction*.
18. Kihiu, J. M. and Masu, L. M. (1995), "The effect of chamfer and size on the stress distributions in thick-walled cylinder with a cross bore under internal pressure", *R & D*, pp. 73–78.
19. Lind, N. C. (1967), *Approximate stress concentration analysis for pressurize branch pipe connections*, ASME, PVP -7.
20. Little, R. E. and Bagci, C. (1965), "Stress analyses of pressurized cylinders", *Engineering research bulletin*, publication No. 145, *Oklahoma state university*.
21. Makulsawatudom, P., Mackenzie, D., and Hamilton, R. (2004), "Stress concentration at crossholes in thick cylindrical vessels", *The journal of strain analysis of engineering design*, Vol. 39, pp. 471–481.
22. Masu, L. M. (1997), "Cross bore configuration and size effects on the stress distribution in thick-walled cylinders", *International journal of pressure vessels and piping*, No. 72, pp. 171–176.
23. FAHEEM, S., & APARNA, P. (2014). *Interpersonal communication skills in academic and scholastic perspective: Barriers and solutions*. *International Journal of Humanities, Arts, Medicine and Sciences*, 2(12), 63–72.
24. Masu, L. M. and Craggs, G. (1992), "Fatigue strength of thick-walled cylinders containing cross bores with blending features", *Proc. InstnMechEngrs*, Vol. 206, pp. 299–309.
25. Moffat, D. G., Mistry, J. and Moore, S. E. (1999). *Effective stress factor correlation equations for piping branch junctions under internal pressure loading*, *Journal of pressure vessel technology*, No. 121, pp. 12–6.
26. Moffat, D. G., Mwenifumbo J. A. M, Xu, S. H., Mistry J. (1991). *Effective stress factors for piping branch junctions due to internal pressure and external moments loads*, *journal of strain analysis*, No. 26, pp. 84–101.
27. Money, H. A. (1968). *Designing flush cylinder to cylinder intersections to withstand pressure*, ASMEPVP— 17.
28. Nagpal, S., Jain, N. and Sanyal, S. (2012), "Stress concentration and its mitigation techniques in flat plate with singularities- A critical review", *Engineering journal*, Vol. 16, issue 1.
29. Nihous, G. C., Kinoshita, C. K. and Masutani, S. M. (2008), "Stress concentration factors for oblique holes in pressurized thick walled cylinders", *Journal of pressure vessel technology*, Vol.130/021202-1. DOI: 10.1115/1.2891915.
30. Nziu, P. K. and Masu, L. M. (2019a), "Cross bore geometry configuration effects on stress concentration in high pressure vessels. A review", *International journal of mechanical and materials engineering*, doi : 10.1186/s40712-019-0101-x
31. Nziu, P. K. and Masu, L. M. (2019b), "Elastic Strength of High Pressure Vessels with a Radial Circular Cross Bore", *International Journal of Mechanical and Production Engineering Research and Development*, Vol. 9, issue 3, pg.1275–1284, doi : 10.24247/ijmperdjun2019133.
32. O'hara, G. P. (1968), "Experimental investigation of stress concentration factors of holes in thick walled cylinders", *watervliet arsenal technical report WVT-6807*.
33. Peters, D. T. (2003), "Effect of blend radius on stress concentration factor of cross bored holes in thick walled pressure vessels", *Conference proceeding on high pressure technology for the future*, Cleveland, Ohio, USA, July 20–24, pp. 53–57.

34. Qadir, M. and Redekop, D. (2009), "SCF analysis of a pressurised vessel-nozzle intersection with wall thinning damage", *International journal of pressure vessels and piping*, Vol. 86, pp. 541–549.
35. Sanyal, S and Yadav, P. (2006), "Relief holes for stress mitigation in infinite thin plate with single circular hole loaded axially", *ASME international mechanical engineering congress and exposition*.
36. Snowberger, D. (2008), "Stress concentration factor convergence comparison study of a flat plate under elastic loading conditions", *Rensselaer Polytechnic Institute Hartford, Connecticut*.
37. Timoshenko, S. (1940), "Strength of materials part II: Advanced theory and problem" Second edition, ninth printing, D. Van Nostrand Company, Inc.
38. Xie, D. and Lu, L. (1985), "Prediction of stress concentration factors for cylindrical pressure vessels with nozzles", *International journal of pressure vessels and piping*, No. 21, pp. 1–20.

AUTHORS PROFILE



Professor LM Masu holds BSc (Hons) Mech.Eng, MSc. Mech.Eng., PhD. (Leeds), PG Dip. B Admin (UDW) and MBA (UFS). He is registered as Pr.Eng (ECSA), FSAIMechE, R Eng (K) and MIEK. Prof Masu has published 51 journal and 33 conferences articles, co-authored 1 book and 1 book chapter. He has a total of 38 years of academic experience, of which 27 years has been on academic managerial levels. In addition to this wealthy experience, Prof Masu has 4 years hands on industrial experience.



Dr. PK Nziu holds BSc (Hons), MTech and DTech in Mechanical Engineering (VUT). He is registered as a candidate Eng.(ECSA) and Member (SAIMechE). He has published a total of 13 journal articles and presented 4 articles in international conferences. Dr Nziu has a total of 10 years academic experience in addition to 3½ years hands on industrial experience.

